PROCEEDINGS OF SCIENCE

Measurement and interpretations of $W^{\pm}Z$ cross-sections in pp collisions at $\sqrt{s}$ = 13 TeV with the ATLAS detector

Léo Boudet[a,*], **on behalf of the ATLAS Collaboration**

[a] *LAPP, Université Savoie Mont Blanc, CNRS/IN2P3*
9 chemin de Bellevue, 74940, Annecy; France

E-mail: leo.boudet@cern.ch

Measurements of integrated and differential cross-sections for $W^{\pm}Z$ production in proton–proton collisions are presented. The data collected by the ATLAS detector at the Large Hadron Collider from 2015 to 2018 at a centre-of-mass energy of $\sqrt{s}$ = 13 TeV are used, corresponding to an integrated luminosity of 140 fb^{-1}. The $W^{\pm}Z$ candidate events are reconstructed using leptonic decay modes of the gauge bosons into electrons or muons. The integrated cross-section for the production of $W^{\pm}Z$ is measured in the detector fiducial region. The $W^{\pm}Z$ production is also measured differentially as functions of various kinematic variables, including new observables sensitive to CP-violation effects. All measurements are compared with state-of-the-art Standard Model predictions from fixed-order calculations or Monte Carlo generators based on next-to-leading-order matrix elements interfaced with parton showers. An effective field theory interpretation of the measurements is performed, considering both CP-conserving and CP-violating dimension-6 operators modifying the $W^{\pm}Z$ production. Limits on CP-conserving Wilson coefficients are extracted using the transverse mass of the $W^{\pm}Z$ system. For CP-violating coefficients a machine learning approach is used to construct an observable with enhanced sensitivity to CP-violation effects.

The European Physical Society Conference on High Energy Physics (EPS-HEP2025)
7-11 July 2025
Marseille, France

[*] Speaker

https://pos.sissa.it/

PoS(EPS-HEP2025)298

1. Interest of $W^{\pm}Z$ inclusive production

This work has been published in Ref. [9] and submitted to JHEP. The $W^{\pm}Z$ inclusive production constitutes an important test of the Standard Model (SM) of particle physics, due to its sensitivity to gauge boson self-interactions which are related to the non-Abelian structure of the electroweak interaction. It provides a means to directly probe the triple gauge boson couplings (TGC), in particular the WWZ gauge coupling, and to look for anomalous couplings.

The study of the leptonic decay of the $W^{\pm}Z$ boson pair process enables precision measurements of its integrated and differential production cross-sections. The measurements on the full LHC Run 2 dataset, recorded by ATLAS [1] at $\sqrt{s}$ = 13 TeV and corresponding to an integrated luminosity of 140 fb^{-1}, are compared with predictions from state-of-the art Monte Carlo (MC) event generators. For this purpose, the most recent calculations at next-to-next-to-leading-order (NNLO) in QCD and next-to-leading-order (NLO) in electroweak (EW) from MATRIX [12–14] are considered.

2. $W^{\pm}Z \rightarrow \ell\nu\ell\ell$ event selection

The W and Z bosons are reconstructed using their decays into electrons or muons. The lepton selection is performed is three successive steps. The baseline selection (loose set of cuts, $p_{\mathrm{T}} \geq 5$ GeV) is folowed by the Z selection (tighter identification cut, $p_{\mathrm{T}} \geq 15$ GeV), finally followed by the W selection: (tighter identification and isolation cuts, $p_{\mathrm{T}} \geq 20$ GeV).

This three steps selection is used to select $W^{\pm}Z$ events and define the Control Regions (CR) of the main backgrounds. The $W^{\pm}Z$ events are required to have exactly three baseline leptons, with at least one satisfying the W selection and two Z-leptons with the same flavour and opposite electric charges satisfying $|m_{\ell\ell} - m_Z| \leq 10$ GeV. The ZZ production is the main irreducible background, controlled with a dedicated CR. The events in this CR must pass the same selection cuts as the $W^{\pm}Z$ ones, except they must contain at least four baseline leptons. The $t\bar{t} + V$ ($V = W^{\pm}$ or Z) control sample is defined as a sub-sample of $W^{\pm}Z$ candidate events with at least two reconstructed b-jets. Events from the electroweak $WZjj$ production ($WZjj$-EW) are considered as backgrounds. Smaller irreducible backgrounds (VVV, tZj, $WZjj$-EW production) are estimated using MC simulations without dedicated CR.

The reducible background events with at least one misidentified lepton, mostly originate from $Z + j$, $Z\gamma$, $t\bar{t}$ and WW production processes. These events are estimated with a data-driven Matrix Method containing the efficiencies and misidentification probabilities for prompt and misidentified leptons [2–4, 7].

3. Inclusive cross-section measurement

The inclusive $W^{\pm}Z$ cross-section is measured separately in each of the four lepton decay channels, then combined into the total cross-section with a χ^2 combination (Figure 1(a)). The inclusive cross-sections are measured for $W^{+}Z$ and $W^{-}Z$ events separately, as well, and their ratio is reported in Figure 1(b) and compared with fixed order SM calculations.

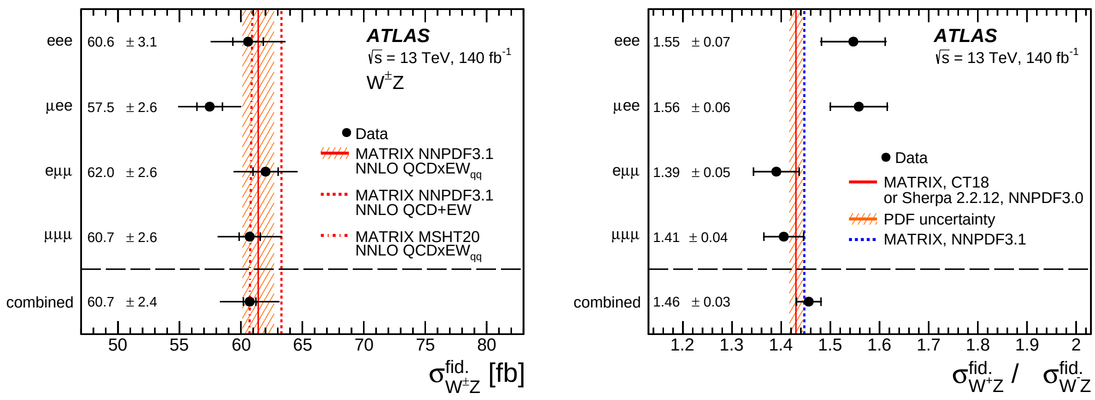

(a) **(b)**

Figure 1: Inclusive $W^{\pm}Z$ cross-section measurements (a) and ratio of the $W^{+}Z$ over the $W^{-}Z$ cross-section (b) in each of the four leptonic channels and their combination, taken from Ref. [9] in all figures.

The total relative uncertainty on the fiducial cross-section is 4.0% (0.8% stat. ⊕ 3.4% syst. ⊕ 1.0% lumi.).

The predictions shown in Figure 1 are provided by MATRIX calculations using the NNLO QCD + NLO EW and NNLO QCD × NLO EW$_{qq}$ schemes. The prediction of the multiplicative scheme describes the data better than the additive one as shown in Figure 1(a). The 2.3% relative uncertainty on the MATRIX prediction is of the same order of experimental uncertainties. The $\sigma^{\text{fid.}}_{W^{+}Z}/\sigma^{\text{fid.}}_{W^{-}Z}$ ratio shown in Figure 1(b) highlights the impact of different Parton Distribution Functions (PDF) sets. The MATRIX calculation with the NNPDF3.1 provides the most accurate description of data among the sets considered. It predicts a slightly higher ratio with respect to the CT18 one or the NNPDF3.0 used by Sherpa 2.2.12.

4. Differential cross-section measurements

Differential cross-sections in several variables are also measured in this work. The transverse momentum of the boson with leading p_{T}, denoted p_{T}^{V1}, is sensitive to the effect of the different schemes used to account NLO EW corrections in the high energy tail (Figure 2(a)). The low energy tail of this distribution shows a discrepancy between data and SM predictions, which is the manifestation of the domination of soft and collinear QCD radiations in this kinematical regime, that cannot be described by the perturbative expansion in the strong coupling constant α_{S}. The azimuthal angle difference between the Z boson and the W decay lepton $\Delta\phi(\ell^{W}, Z)$ is presented in order to highlight the differences between the predictions of the PowHeg+Pythia8 and Sherpa 2.2.12 predictions, the latter being favored by data.

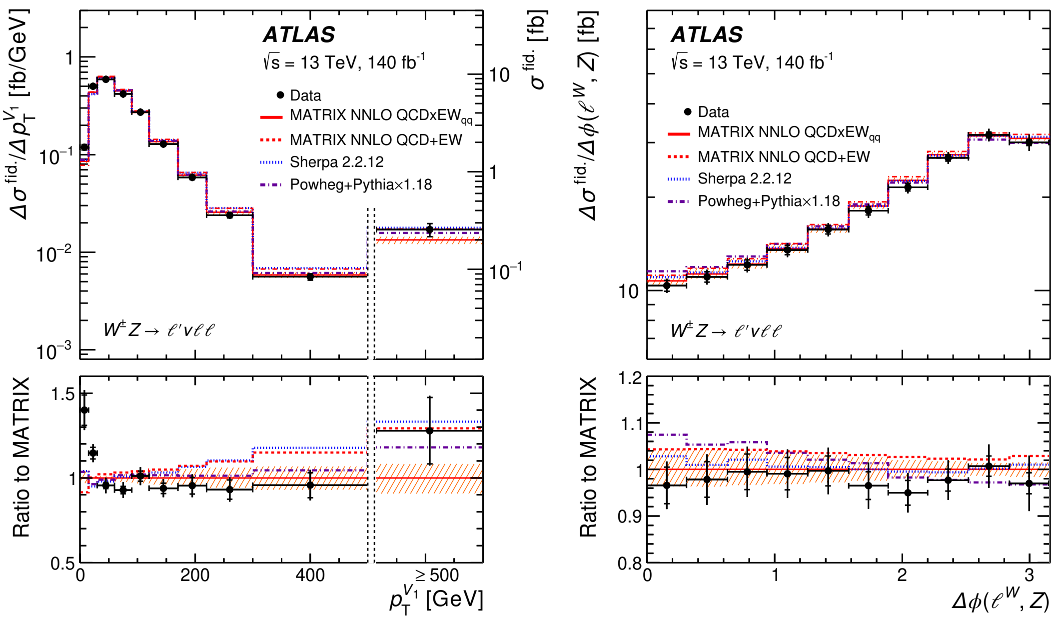

(a) **(b)**

Figure 2: Differential cross-section measurements for p_{T}^{V1} (a) and $\Delta\phi(\ell^W, Z)$(b), taken from Ref. [9] in all figures.

5. EFT interpretation

The measured detector-level distributions are used to constrain Wilson coefficients of dimension-6 operators of the SM effective field theory (SMEFT), described by the Lagrangian

$$\mathcal{L}_{SMEFT} = \mathcal{L}_{SM} + \sum_{n\geq 5} \sum_{i} \frac{c_i^{(n)}}{\Lambda^{n-4}} O_i^{(n)} , \qquad (1)$$

where Λ represents the new physics energy scale of the theory and $c_i^{(n)}$ are the Wilson coefficients attached to each operator $O_i^{(n)}$. The considered coefficients of the theory impact the couplings between vector bosons and incoming quarks ($c_{Hq}^{(1)}$, $c_{Hq}^{(3)}$) and the TGC (c_{HD}, c_W, c_{HWB} and the CP-violating counterparts $c_{\tilde{W}}$, $c_{H\tilde{W}B}$). The decomposition method is used to perform a maximum likelihood fit of the parameters of interest c_i/Λ^2. The EFT Monte Carlo predictions are generated using MadGraph5 interfaced with the SMEFTSim package [11].

For the CP-conserving SMEFT operators, a fit on the m_{T}^{WZ} distribution is performed, as the high energy tail is sensitive to any EFT quadratic contribution. The binning of the distribution is optimised for this purpose. For the CP-violating operators, a novel multivariate approach is used, to exploit the asymmetric shape of the EFT linear contribution. For each CP-violating operator, a set of three Boosted Decision Trees is trained to perform three binary discriminations between the events of the SM Monte Carlo simulation, the positively weighted events of the linear EFT term simulation and the negatively weighted ones. The three resulting BDT scores are combined into a final observable noted S_{comb}, designed to present a symmetric shape around zero for CP-conserving terms and to enhance the asymmetry of the linear EFT term. This variable is split into a low and a high energy region ($m_{\mathrm{T}}^{WZ} \lessgtr 600$ GeV), the latter being sensitive to the quadratic EFT contribution. Confidence limits at the 95% level are extracted from a maximum likelihood fit and are shown in Figure 3 with only one non-zero Wilson coefficient at a time. The multivariate approach improves the stringency of the limits by a factor up to 2.9 for $c_{H\tilde{W}B}/\Lambda^2$.

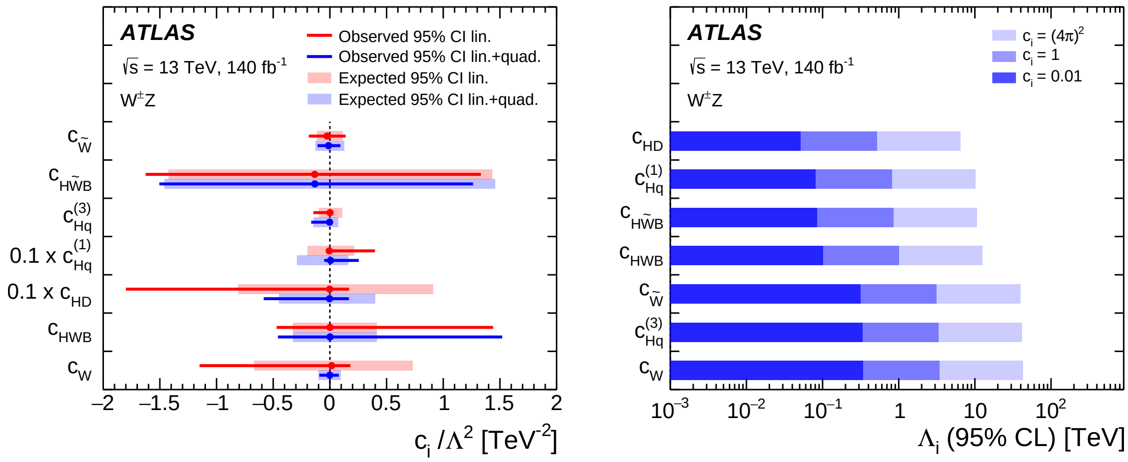

(a) **(b)**

Figure 3: Expected (blue) and observed (red) 95% confidence limits on the Wilson coefficients, without ('lin.') and with ('lin.+quad.') the quadratic EFT term included in the fit (a). The limits are interpreted in terms of constraints on the new physics energy scale Λ (b), taken from Ref. [9] in all figures.

All limits shown in Figure 3(a) are compatible with the Standard Model at the 95% confidence level. The limits on the CP-violating Wilson coefficients are competitive with other state-of-the art ATLAS constraints [5, 6, 8, 10]. The limits put on the c_i/Λ^2 ratios are interpreted in Figure 3(b) as limits on the energy scale of new physics Λ for different fixed values of the Wilson coefficients corresponding to scenarios of different coupling strengths between the SM and potential BSM fields.

PoS(EPS-HEP2025)298

References

[1] ATLAS Collaboration
The ATLAS Experiment at the CERN Large Hadron Collider.
JINST **3** (2008) S08003

[2] ATLAS Collaboration [ATLAS Collaboration]
Search for supersymmetry at $\sqrt{s}$=8 TeV in final states with jets and two same-sign leptons or three leptons with the ATLAS detector.
JHEP **06** (2014) 035 [arXiv: 1404.2500]

[3] ATLAS Collaboration
Measurements of $W^{\pm}Z$ production cross sections in pp collisions at $\sqrt{s}$ = 8 TeV with the ATLAS detector and limits on anomalous gauge boson self-couplings.
Phys. Rev. **D93** 9, (2016) 092004 [arXiv: 1603.02151]

[4] ATLAS Collaboration
Measurement of $W^{\pm}Z$ production cross sections and gauge boson polarisation in pp collisions at $\sqrt{s} = 13$ TeV with the ATLAS detector.
Eur. Phys. J. **C79** 6, (2019) 535 [arXiv: 1902.05759]

[5] ATLAS Collaboration
Differential cross-section measurements for the electroweak production of dijets in association with a Z boson in proton–proton collisions at ATLAS.
Eur. Phys. J. **C81** 2, (2021) [arXiv: 2006.15458]

[6] ATLAS Collaboration
Integrated and differential fiducial cross-section measurements for the vector boson fusion production of the Higgs boson in the $H \rightarrow WW^{*} \rightarrow e\nu\mu\nu$ decay channel at 13 TeV with the ATLAS detector.
Phys. Rev. **D108** 7, (2023) [arXiv: 2304.03053]

[7] ATLAS Collaboration [ATLAS Collaboration]
Tools for estimating fake/non-prompt lepton backgrounds with the ATLAS detector at the LHC.
JINST **18** 11, (2023) T11004 [arXiv: 2211.16178]

[8] ATLAS Collaboration
Differential cross-section measurements of Higgs boson production in the $H \rightarrow \tau^{+}\tau^{-}$ decay channel in pp collisions at $\sqrt{s}$ = 13 TeV with the ATLAS detector.
JHEP **03** (2025) 010 [arXiv: 2407.16320]

[9] ATLAS Collaboration
Measurements and interpretations of $W^{\pm}Z$ production cross-sections in pp collisions at $\sqrt{s}$ = 13 TeV with the ATLAS detector.
(2025) [arXiv: 2507.03500]

[10] ATLAS Collaboration
Measurements of Higgs boson production via gluon-gluon fusion and vector-boson fusion using $H \to WW^* \to \ell\nu\ell\nu$ decays in pp collisions with the ATLAS detector and their effective field theory interpretations.
(2025) [arXiv: 2504.07686]

[11] Ilaria Brivio, Yun Jiang, and Michael Trott
The SMEFTsim package, theory and tools.
JHEP **12** (2017) [arXiv: 1709.06492]

[12] Massimiliano Grazzini, S. Kallweit, Jonas M. Lindert, Stefano Pozzorini, and Marius Wiesemann
NNLO QCD + NLO EW with Matrix+OpenLoops: precise predictions for vector-boson pair production.
JHEP **02** (2020) 087 [arXiv: 1912.00068]

[13] Massimiliano Grazzini, Stefan Kallweit, Dirk Rathlev, and Marius Wiesemann
$W^{\pm}Z$ production at the LHC: fiducial cross sections and distributions in NNLO QCD.
JHEP **05** (2017) 139 [arXiv: 1703.09065]

[14] M. Grazzini, S. Kallweit, D. Rathlev and M. Wiesemann
$W^{\pm}Z$ production at the LHC: fiducial cross sections and distributions in NNLO QCD.
JHEP **05** (2017) [arXiv: 1703.09065]